Mon. Not. R. astr. Soc. (1970) **151**, 65–80.

INTERNAL STRUCTURE OF UPPER MAIN-SEQUENCE STARS

R. Stothers

(Communicated by H.-Y. Chiu)

(Received 1970 August 3)

SUMMARY

In main-sequence stars heavier than 9 $M_\odot$, convective instability develops just outside the zero-age convective core as hydrogen depletion proceeds. At least ten schemes are available in the literature to treat the unstable intermediate zone which results. A detailed investigation is presented here, utilizing physical, laboratory, stellar-model, and observational considerations. Only two schemes survive, both of which are semiconvective: the modified Schwarzschild–Härm (SH) prescription and the modified Ledoux–Sakashita–Hayashi (LSH) prescription. The former scheme is tentatively favoured by the weight of laboratory evidence. In either case, the earliest stages of hydrogen depletion are characterized by a semiconvective zone which joins continuously the convective core and the outer radiative envelope. The later stages are characterized by a radiative detachment of the semiconvective zone from the core, except for masses above 15 $M_\odot$ in the SH scheme. At any given mass, the final hydrogen profiles resulting from each of the two schemes are very similar.

1. INTRODUCTION

Considerable controversy has arisen regarding the correct criterion to use for stability against convection in a region of a star which possesses a gradient of mean molecular weight. On rough physical grounds, Ledoux (1947) and Sakashita, Ono & Hayashi (1959) argued that the criterion should be based on a comparison of the local 'radiative' and 'adiabatic' *density gradients* (in accordance with the original criterion of K. Schwarzschild), which leads directly to

$$\nabla_{\rm rad} < \nabla_{\rm ad} + \frac{\beta}{4-3\beta}\frac{d\ln\mu}{d\ln P}. \qquad (1)$$

Here we have used the following definitions:

$$\nabla = d\ln T/d\ln P, \qquad \beta = P_{\rm gas}/(P_{\rm gas}+P_{\rm rad}),$$

$$\nabla_{\rm rad} = \frac{\kappa L(r)}{16\pi cGM(1-\beta)q}, \qquad \nabla_{\rm ad} = \frac{8-6\beta}{32-24\beta-3\beta^2},$$

for a fully ionized gas with mean molecular weight μ located at mass fraction q in the star. However, Schwarzschild & Härm (1958) presented an alternative argument in favour of a more stringent criterion based on a comparison of the *temperature gradients*:

$$\nabla_{\rm rad} < \nabla_{\rm ad}. \qquad (2)$$

In either case, violation of the adopted criterion implies the outbreak of convective motions. The new distribution of chemical composition which is set up by the convective mixing may or may not depend on the adopted criterion. If a region of a star is in stable radiative equilibrium in the sense of criterion (2), it is necessarily so in the sense of criterion (1), but the converse is not always true. Such a complex situation arises prominently in the evolution of massive main-sequence stars, and the regions where criterion (1) or (2) is disobeyed and the character of the resulting mixing are the subject of the present paper.

Some basic conclusions can be arrived at from primarily physical considerations. However, laboratory experiments and actual construction and testing of stellar models are naturally indispensable. And, ultimately, stellar observational data must be reproduced by the models. The interesting possibility arises that one might be able to infer the character of the convective mixing from (a) the mere requirement of being able to fit self-consistent stellar models and (b) comparison of such models with the relevant observational data. The major part of this paper is devoted to such an attempt, based on available published models and a considerable number of new models. Although rotation will be neglected, one should keep in mind that rotational mixing currents will alter, to some extent, the character of the convective mixing.

2. PHYSICAL CONSIDERATIONS

It is generally understood that the boundary between a fully convective region and a region which is in complete or partial radiative equilibrium is governed by the condition

$$\nabla_{\rm rad} = \nabla_{\rm ad}, \tag{3}$$

which is to hold on the side of the boundary which contains the fully convective region (Ledoux 1947; Kippenhahn 1963; Unno 1965). This is necessary in order to ensure that the convective velocity of turbulent elements in the unstable layer goes to zero at the boundary, minimizing convective overshooting into the stable radiative layers. Condition (3) applies whether the fully convective region is advancing or retreating.

In a massive star, conversion of hydrogen into helium in the convective core is accompanied by a monotonic rise in luminosity and relative radiation pressure (due to the increase in mean molecular weight of the gas). The percentage increase in luminosity is larger than the percentage increase in relative radiation pressure since $1-\beta$ is *ab initio* a large fraction of unity ($\nabla_{\rm ad} \approx 0{\cdot}25$). Hence, convective instability grows outward in mass fraction, as indicated by equation (3) rewritten in the form

$$q_f = \left(\frac{\kappa \nabla_{ad}^{-1}}{16\pi cGM} \frac{L}{1-\beta} \right)_f. \tag{4}$$

If the convectively unstable region is mixed homogeneously to the centre, a composition discontinuity will develop between it and the radiative envelope as central hydrogen is converted into helium.* Since the energy is generated near the stellar centre, well within the boundary of the convective core, the flux must

* It should be noted that, in stars of small mass where β is close to unity ($\nabla_{\rm ad} \approx 0{\cdot}40$), the convectively unstable region rapidly shrinks according to equation (4). Clearly in this case, the retreating convective core leaves behind a region in radiative equilibrium with a smoothly varying μ gradient.

be conserved at the boundary between core and envelope. To avoid an infinite flux at this boundary, the temperature must be continuous. Similarly, to avoid an infinite acceleration of the matter, the pressure must be continuous. Continuity of T and P imply the continuity of β and ρ/μ, through the equation of state. Therefore, according to the definition of $\nabla_{\rm rad}$, the quantity $\nabla_{\rm rad}/\kappa$ also must be the same on the interior and exterior sides of the boundary:

$$\left(\frac{\nabla_{\rm rad}}{\kappa}\right)_{\rm int} = \left(\frac{\nabla_{\rm rad}}{\kappa}\right)_{\rm ext}. \tag{5}$$

For an opacity source of Kramers type, one has $\kappa \sim (1+X)\rho \sim (1+X)\mu$, where X is the fractional abundance of hydrogen by mass. Since $\mu \sim (1+X)^{-1\cdot4}$ for a fractional metals abundance Z which is small, one finds $\kappa \sim (1+X)^{-0\cdot4}$. Since $X_{\rm int} \leq X_{\rm ext}$, equation (5) implies that $(\nabla_{\rm rad})_{\rm ext} \leq (\nabla_{\rm rad})_{\rm int}$ and, therefore, that the exterior side is in strongly radiative equilibrium, as assumed. So the convective core can grow in mass fraction if the local opacity source is Kramers-like.

In massive stars, however, the opacity is due primarily to electron scattering, in which case $\kappa = 0\cdot2\ (1+X)$. Equation (5) then implies that the exterior side of the core boundary is in convective equilibrium, contrary to the assumption. It is generally agreed (e.g., Schwarzschild & Härm 1958; Sakashita *et al.* 1959) that this contradiction demonstrates that the convective core (and, indeed, *any* fully convective region having a smaller hydrogen abundance X than has the contiguous radiative region) cannot grow into radiative layers if the local opacity source is electron scattering. Since a variety of schemes have been proposed for coping with this difficulty, it is intended here to examine these schemes critically in terms of our present combined knowledge of the relevant hydrodynamics (laboratory and theoretical), stellar model construction, and stellar observations. This seems the only way to resolve the difficulty at present since the requirement of mathematical consistency alone does not appear to lead to a unique evolutionary sequence of models, as Tayler (1969) has stressed.

The main question that arises is the nature of the convectively unstable region that is left behind by the retreating convective core. This unstable region will, of course, contain a gradient of mean molecular weight, which tends to choke off convection as indicated by inequality (1); the region will be therefore *slowly* mixed until convective neutrality is attained. The convective mixing readjusts the distribution of chemical composition such that lighter material is transported downward and heavier material upward. This process has been termed 'semi-convection' by Schwarzschild & Härm (1958). The state of convective neutrality is reached when an equality obtains either in condition (1), as adopted by Ledoux and Sakashita & Hayashi:

$$\nabla_{\rm rad} = \nabla_{\rm ad} + \frac{\beta}{4-3\beta}\frac{d\ln\mu}{d\ln P} \qquad \text{(LSH)}; \tag{6}$$

or in condition (2), as adopted by Schwarzschild & Härm:

$$\nabla_{\rm rad} = \nabla_{\rm ad} \qquad \text{(SH)}. \tag{7}$$

Arguments of a mathematical nature have been advanced in favour of prescription (1) and (6) by Gabriel (1969) and prescription (2) and (7) by Kato (1967).

However, at least ten schemes are available in the literature to treat in detail the convectively unstable region which develops during core hydrogen depletion.

In all of these schemes, the outer envelope is found to be in radiative equilibrium down to the point closest to the surface at which $\nabla_{rad} = \nabla_{ad}$. However, the inner core is only *assumed* to be in convective equilibrium (and therefore chemically homogeneous) out to the point closest to the centre at which chemical inhomogeneity begins (for inhomogeneous models); in some of the schemes, it is found that $\nabla_{rad} < \nabla_{ad}$ at this point, but the *innermost* regions of the core are always found to be in convective equilibrium.

In the following discussion, the different schemes will be briefly described, with a comment as to their physical self-consistency and with occasional references to the published literature where necessary. For ease in description, Fig. 1 has been prepared, showing the hydrogen profile $X(q)$ for each scheme in the case of a typical star of high mass near the end of core hydrogen burning. Solid and dashed lines refer to regions where it is formally found that $\nabla_{rad} < \nabla_{ad}$ and $\nabla_{rad} > \nabla_{ad}$, respectively; a dot marks a point where $\nabla_{rad} = \nabla_{ad}$ identically. The sporadic violation of criterion (2) in the 'radiative' zone immediately above the convective core in schemes R, M1, M2, and possibly N1 and N2 is not indicated in Fig. 1; but criterion (1) is never violated in this zone. Semicircular marks denote a zone in which the temperature gradient has been taken to be adiabatic (∇_{ad}). Leftward (\\\) or rightward (///) hatch marks denote a semiconvective zone where the chemical composition at each point has been evaluated according to equation (6) or (7), respectively; in each case, the temperature gradient has been taken to be the radiative one (∇_{rad}) because of the inefficiency of the semiconvective motions in transporting flux. Discussion of the individual schemes now follows.

Scheme R. All layers outside the instantaneous convective core are assumed to be radiative (no mixing) in calculating the μ gradient. Thus, the chemical composition is assumed to be 'frozen in' as the convective core retreats. The core boundary is defined as the point closest to the centre where $\nabla_{rad} = \nabla_{ad}$, in the normal fashion. In all layers where criterion (2) is disobeyed, the temperature gradient is taken to be the adiabatic one. Clearly, this scheme is non-physical since it ignores the mixing implied by violation of criterion (1) or (2) in regions outside the core.

Scheme H. The star is assumed to evolve completely mixed, so that the chemical composition is, at all times, homogeneous throughout. The temperature gradient is taken to be the smaller of ∇_{rad} and ∇_{ad}, as in the case of a zero-age main-sequence star. Complete mixing of the evolving star is clearly non-physical (in the absence of rotation) since the envelope is always found to be in radiative equilibrium.

Scheme C1. The convective core is assumed to grow out in mass fraction as evolution proceeds. The chemical discontinuity at the boundary with the radiative envelope is placed at the point in the envelope closest to the stellar surface where $\nabla_{rad} = \nabla_{ad}$. However, the jump in hydrogen content leads to $\nabla_{rad} < \nabla_{ad}$ at the interior side of the boundary, and the core is not wholly convective as assumed. The solution is therefore non-physical.

Scheme C2. A homogeneous, convective intermediate zone with intermediate hydrogen content is placed between the radiative envelope and convective core. The resulting chemical discontinuities at the two boundaries of this zone are located at the points where $\nabla_{rad} = \nabla_{ad}$ on the exterior side of each boundary. However, the solution is non-physical for the same reason given for scheme C1.

Placement of the chemical discontinuities in schemes C1 and C2 at the points

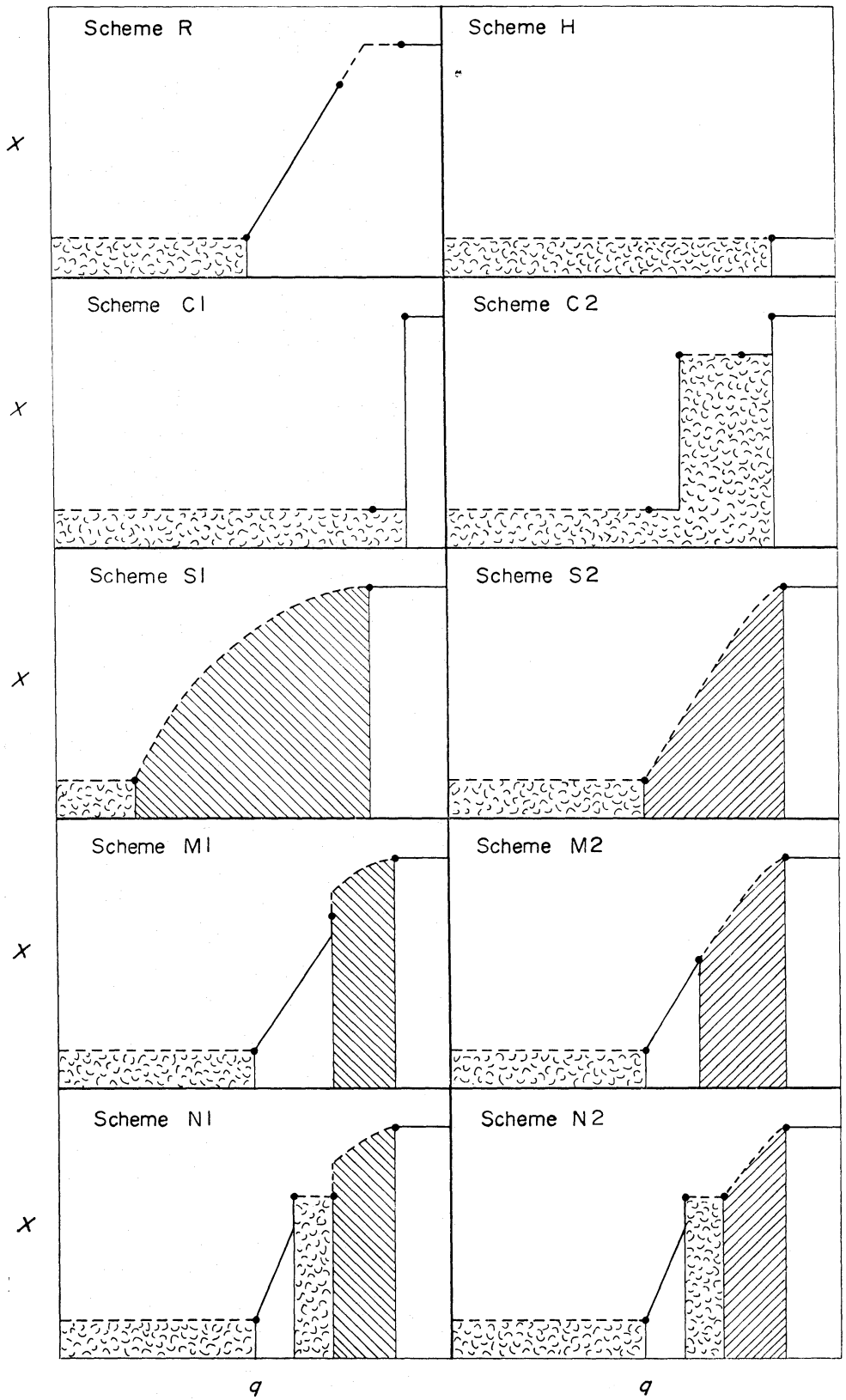

FIG. 1. *Hydrogen profile in very massive stars near the end of core hydrogen burning, for ten schemes of evolution. Meaning of notation:* $\nabla_{rad} < \nabla_{ad}$ *(solid lines);* $\nabla_{rad} > \nabla_{ad}$ *(dashed lines);* $\nabla_{rad} = \nabla_{ad}$ *(dot);* $\nabla = \nabla_{ad}$ *(semicircular marks);* $\nabla_{rad} \approx \nabla_{ad} + \beta(4-3\beta)^{-1}$ *d ln* μ*/d ln P (leftward hatching* *);* $\nabla_{rad} \approx \nabla_{ad}$ *(rightward hatching* ////*);* $\nabla = \nabla_{rad}$ *(elsewhere). The criterion* $\nabla_{rad} < \nabla_{ad}$ *is sporadically disobeyed in the innermost 'radiative' zone of schemes R, M1, M2, and possibly N1 and N2.*

where $\nabla_{rad} = \nabla_{ad}$ on the *interior* sides of the boundaries is meaningless, since, in this case, the jump in hydrogen content implies $\nabla_{rad} > \nabla_{ad}$ along the interface and above it. Thus an exterior convective zone is implied, containing a chemical discontinuity, which is physically impossible.

Scheme S1. A semiconvective zone obeying the LSH prescription is placed between the radiative envelope and convective core. Equation (6) yields the chemical composition at each point in the semiconvective zone, and the zonal boundaries are defined by the points at which $\nabla_{rad} = \nabla_{ad}$. Since the μ gradient is very shallow at the upper boundary, no difficulty is encountered in determining the mass fraction of this boundary. However, a very rapid change in the μ gradient must occur in the neighbourhood of the core boundary in order that this gradient vanish precisely at the core boundary (Kippenhahn 1963; Uchida, Suda & Hitotuyanagi 1967). This feature of the μ gradient can remove the inconsistency of a flux discontinuity found earlier by Sakashita & Hayashi (1959, 1961). However, for computational purposes, the very narrow zone of rapid change can be replaced by a *discontinuity* of the μ gradient, leaving μ itself continuous; therefore, on the exterior side of the core boundary, equation (6) applies while, on the interior side, $\nabla_{rad} = \nabla_{ad}$. Everywhere outside the convective core the temperature gradient is assumed to be the radiative one.

Scheme S2. This scheme is analogous to scheme S1, except that the SH prescription is adopted for the semiconvective zone. Equation (7) yields the chemical composition at each point in the semiconvective zone. No difficulty is encountered in determining the mass fraction of the inner boundary of this zone because $\nabla_{rad} = \nabla_{ad}$ everywhere in the zone.

Scheme M1. A hybrid, this scheme was originally set up by Sakashita & Hayashi (1961) in order to circumvent the inconsistency which they thought to be present in scheme S1. Between the LSH semiconvective zone and the convective core, a radiative zone is placed. At all points in the radiative zone, criterion (1) is found to be obeyed although criterion (2) may not be. The chemical composition of the radiative zone is determined in the same way as for the case of scheme R. The upper boundary of the radiative zone is marked by a chemical discontinuity with the semiconvective zone; the latter zone is found to grow in mass fraction during evolution, thereby causing the development of the steep μ gradient (approximated as a discontinuity) at its interface with the underlying radiative zone. The mass fraction of this interface is determined by requiring that the integrated hydrogen content in regions away from the shrinking convective core be conserved during evolution (because of the lack of nuclear burning in these regions). The temperature gradient is taken to be radiative everywhere outside the convective core.

Scheme M2. This scheme is analogous to scheme M1, except that the SH prescription is adopted for the semiconvective zone. No chemical discontinuity occurs at the interface with the underlying radiative zone because $\nabla_{rad} = \nabla_{ad}$ throughout the semiconvective zone. However, to conserve the total amount of unburned hydrogen outside the convective core, it is necessary to increase secularly the hydrogen content at some points within the inner radiative (stable) zone. In the absence of overshooting mass motions from the semiconvective zone, this is a physical impossibility.

Scheme N1. A complicated hybrid, this scheme combines features of schemes M1 and C2 by adopting a fully convective (chemically homogeneous) zone between the semiconvective zone and inner radiative zone of scheme M1 (Stothers 1966a).

The chemical composition of the intermediate convective zone is determined by requiring (a) $\nabla_{rad} = \nabla_{ad}$ at each of the two boundaries of the zone, and (b) conservation of the integrated hydrogen content in regions away from the shrinking convective core. These specifications imply the necessity of chemical discontinuities at both boundaries of the new zone. The size of the jump in hydrogen content at the outer boundary is automatically governed by the requirement that equation (6) apply on the exterior (semiconvective) side of the discontinuity and $\nabla_{rad} = \nabla_{ad}$ on the interior side. The actual placement of the outer boundary is governed by the requirement of conservation of the integrated hydrogen content in regions away from the convective core; the placement of the inner boundary is automatically made at the point where $\nabla_{rad} = \nabla_{ad}$ on the exterior (convective) side of the boundary. Since the fully convective zone grows *inward* into a radiative region of smaller hydrogen abundance X during evolution, no physical contradiction is implied, unlike the case of scheme C2. The temperature gradient is taken to be radiative everywhere except in the convective core and in the intermediate convective zone.

It should be remarked that the chemical discontinuity at the semiconvective–convective interface in scheme N1 can be removed by hypothesizing the existence of a rapidly changing μ gradient there (as in the case of scheme S1). Since, in such a case, the change in μ itself is small near the interface, it is *not* represented by a chemical discontinuity.

Scheme N2. This scheme is analogous to scheme N1, except that the SH prescription is adopted for the semiconvective zone and therefore no chemical discontinuity ever occurs at the semiconvective–convective interface.

Careful inspection reveals no obvious self-contradiction in the set-up of

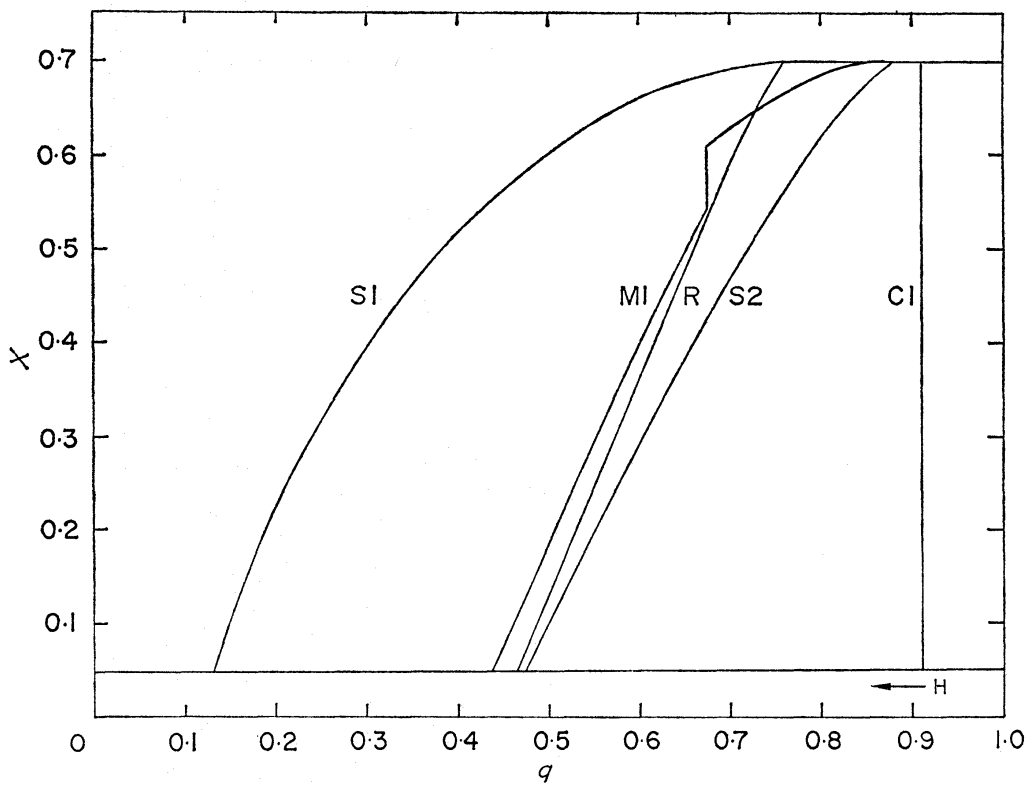

FIG. 2. *Hydrogen profile in a star of* 60 $M_\odot$ *near the end of core hydrogen burning, for six schemes of evolution.*

schemes S1, S2, M1, N1, or N2. However, schemes R, H, C1, C2, and M2 do not appear to be physically self-consistent, although scheme M2 can conceivably apply if convective overshooting occurs efficiently. A possible advantage of schemes N1 and N2 over schemes M1 and M2 is that they *may* avoid the violation of criterion (2) (if this is the proper criterion to use) in the inner radiative zone, but this is not certain. Furthermore, when hydrogen is exhausted in the core, convection near the centre practically vanishes, a radiative shell of hydrogen ignites, and the semiconvective zone of schemes S1 and S2 must eventually retreat; then one of the hybrid schemes is undeniably necessary to follow the further evolution.

Fig. 2 shows the final hydrogen profile resulting from six of the above schemes in the case of a star of 60 $M_\odot$, where the schemes are expected to diverge most strongly from each other. Here, as in other models calculated in this paper, we have adopted a standard set of initial chemical parameters: $X_e = 0{\cdot}70$, $Z_e = 0{\cdot}03$, $Z_e/X_{\rm CNO} = 2$, and electron-scattering opacity. Scheme C2 is not shown since its development is non-unique. Schemes M2, N1, and N2 have not been calculated, but the hydrogen profile for scheme M2 is expected to lie between the profiles calculated for schemes S2 and R.

3. MODEL CONSIDERATIONS

Minimum mass

Attention is first directed to the precise mass at which instability just outside the core boundary manifests itself before the end of core hydrogen burning. The critical mass is sensitive to chemical composition through the mean molecular weight, but not particularly through the opacity as long as the metals abundance is small. For a purely electron-scattering opacity, stellar models admit a homology transformation which leaves non-dimensional quantities constant, given by $M\mu_e^2 =$ constant. The critical mass of interest here for electron-scattering opacity is

$$M/M_\odot = 3{\cdot}6\ \mu_e^{-2}$$

(Schwarzschild & Härm 1958), i.e. 10 $M_\odot$ in the case of our standard chemical composition. For the full opacity, the critical mass is 9 $M_\odot$ (Percy 1970). In less massive stars, the entire intermediate zone is always in stable radiative equilibrium, and scheme R applies consistently, as first shown by Tayler (1954) and Kushwaha (1957).

Earliest stages of evolution

The detailed results of stellar models indicate that the convective cores have their largest extent on the *zero-age* main sequence. In the range of stellar masses 10–1000 $M_\odot$, the zero-age cores encompass 1–7 density scale heights (increasing with stellar mass). By the end of core hydrogen burning, the cores have shrunk to only 1–2 density scale heights while the intermediate zones have grown to 1–7, respectively. It is quite likely that, because of the shallow density gradient in the intermediate zone during the earliest stages of core hydrogen burning, overshooting mass motions at the core boundary mix this zone smoothly between core and envelope. Scheme S1 or S2 is clearly indicated for these earliest stages of evolution (Schwarzschild & Härm 1958; Sakashita & Hayashi 1959; Van der Borght 1964; Uchida *et al.* 1967).

Later stages of evolution—imposed solutions

The later stages of evolution are more controversial. We shall begin with a discussion of schemes that have been formally imposed on the unstable intermediate zone.

Using scheme S2 explicitly, Savedoff & van Dyck (1959) found a paradox in stellar models for 10 $M_\odot$ near the end of core hydrogen burning. Within the computed semiconvective zone, the hydrogen content at each point was found to decrease secularly in the proper physical fashion except in the middle of the zone where it began to increase. The resolution of this paradox is clearly that the middle of the zone has become radiative (stable) in time. Savedoff and van Dyck suggested tentatively that overshooting mass motions from the overlying semiconvective layers might augment the hydrogen content of the radiative zone and penetrate to the convective core below. Since only about one density scale height separates the semiconvective zone and convective core, this suggestion has some merit for stars which are not too massive and have small intermediate zones. New calculations by the author show that the paradox discovered by Savedoff and van Dyck vanishes at 15 $M_\odot$ (for the end of core hydrogen burning). Thus scheme S2 may possibly evolve into scheme M2, in the mass range 10–15 $M_\odot$. Alternatively, if the chemical composition of the inner radiative zone becomes truly 'frozen in' as the core shrinks, then scheme N2 is indicated in order to conserve the unburned hydrogen content outside the core.

In the mass range from 15 $M_\odot$ up to the highest masses, scheme S2 appears to be entirely self-consistent, according to calculations by the author, supplemented by those of Schwarzschild & Härm (1958).

The lower mass limit for valid solutions based on scheme S1 seems to be slightly larger than in the case of scheme S2. Sakashita & Hayashi (1959) originally showed that no solution at all exists for partially hydrogen-depleted stars whose mass would be about 12 $M_\odot$ for our standard chemical composition. New calculations by the author demonstrate that solutions for the *final* stages of core hydrogen burning first begin to appear around $\sim$25 $M_\odot$ (the precise mass is difficult to determine) and are then obtainable up to the highest masses. For masses lower than $\sim$25 $M_\odot$, scheme M1 or N1 is indicated.

Apart from their usefulness in the mass range immediately above 9 $M_\odot$, the hybrid schemes M1 and N2 (and probably N1) appear, in all calculated cases, to be self-consistent up to the highest masses. This is definitely known in the case of scheme M1 (Sakashita & Hayashi 1961; Stothers 1963, 1965, 1966b). Scheme N2 also appears to be self-consistent at least in the range 20–50 $M_\odot$ for which calculations are available (Kippenhahn 1969; Morris 1969; Chiosi & Summa 1970, unpublished).

Moreover, the hybrid schemes are essential for the *later* stages of evolution. At the end of core helium burning in models for 30 $M_\odot$ and higher, the author has found that scheme M1, adopted for the earlier stages of evolution, has to be replaced by scheme N1 (Stothers 1966a; Stothers & Chin 1968). However, at 15 $M_\odot$, convective instability is found to disappear entirely from all of the intermediate zones, regardless of their previous history (Iben 1966; Stothers 1968).

For completeness, we should remark that scheme R, while apparently nonphysical above 9 $M_\odot$, is simple to calculate and yields a hydrogen profile at 15 $M_\odot$ (see also Hartwick 1967; Paczynski 1967) which is similar to that given by schemes S2 and M1. Tayler (1969), however, has found a solution using scheme R which

is apparently physical for stars whose mass would be about 16 $M_\odot$ for our standard chemical composition. In his models (dating from 1953), the convectively unstable portion of the envelope lies entirely outside the zero-age convective core and therefore can be realistically treated as fully convective. However, modern calculations by the present author and other authors indicate that the convectively unstable portion is always partially inside the original boundary of the convective core. The reason for the discrepancy apparently resides in the necessary simplifications adopted by Tayler in 1953 to construct his stellar models (cf. Tayler 1954, 1956). Nevertheless, the present author has determined that scheme R can be *formally* applied from 10 $M_\odot$ up to the highest masses, and that the resulting hydrogen profile lies between the profiles yielded by schemes S2 and M1 (cf. Fig. 2).

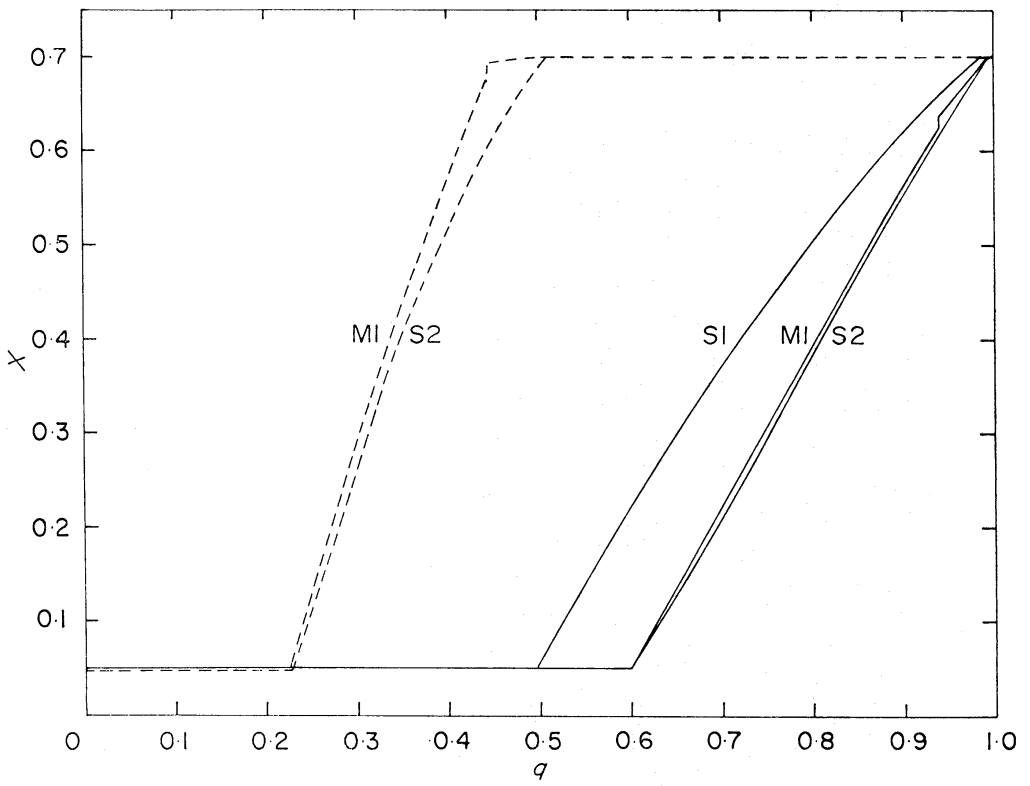

FIG. 3. *Hydrogen profile in stars of* 15 $M_\odot$ (*dashed lines*) *and* 1000 $M_\odot$ (*solid lines*) *near the end of core hydrogen burning, for three schemes of evolution. Scheme S1 does not exist for* 15 $M_\odot$.

Fig. 3 shows the final hydrogen profiles based on schemes R, S1, S2, and M1 for stars of 15 and 1000 $M_\odot$. Throughout the whole range of intervening masses, schemes R, S2, M1, and presumably M2 yield very similar profiles. Indeed, these profiles virtually coincide with each other at 15 $M_\odot$ and again at very high masses, deviating most at 60 $M_\odot$ as shown by Fig. 2. In the limit as the mass becomes infinite, schemes R, S1, S2, M1, and M2 do, in fact, exactly coincide, having a diagonal hydrogen profile, as do schemes H and C1, having a horizontal hydrogen profile.

Later stages of evolution—automatic solutions

Automatic computer programs can sometimes find a solution which simulates mixing, but these solutions are occasionally non-physical (see below) and therefore cannot be uniformly trusted.

Using an automatic program, Henyey, LeLevier & Levee (1959) and Ezer & Cameron (1967) found convective instability occurring in a small zone separated from the core toward the end of core hydrogen burning in stars of 20–100 $M_\odot$. Ezer & Cameron treated the instability by semiconvective mixing according to the SH prescription and simulated scheme M2. Not unexpectedly, the extent of the semiconvective zone and other model parameters agreed well with those of Stothers (1966b), who used the similar scheme M1 explicitly.

In contrast, Hoyle (1960) found that his automatic program unexpectedly produced semiconvective mixing approximating very well the Schwarzschild–Härm scheme S2 in a star of 30 $M_\odot$. Since Blackler (1958) used a program identical to Hoyle's, her models for 32 $M_\odot$ are presumably very similar to his.

But Blackler's published evolutionary tracks for 64 and 128 $M_\odot$ show a discrepant initial *increase* of effective temperature on the H–R diagram, analogous to the increase customarily found around 1 $M_\odot$. From this comparison and from her remark that convectively unstable regions were assumed to be well mixed, we can infer that the homogeneous cores of her most massive models were initially *growing* in mass fraction and simulating scheme C1. The models of Levee & Hilton (1959), for a star whose mass would be about 13 $M_\odot$ for our standard chemical composition, also appear to simulate scheme C1. Iben's (1966) automatic program was coded to assume complete mixing in unstable regions, but it produced in 15 $M_\odot$ three fully convective regions of different mean molecular weight—the convective core and two convective intermediate zones which blended into one after core hydrogen exhaustion; this set-up resembles scheme C2, but is not exactly equivalent.

According to our earlier discussion of schemes C1, C2, and M2, it is likely that the models of Ezer & Cameron, Blackler, Levee & Hilton, and Iben are non-physical, even though the machine found mathematical solutions. Moreover, in the models of Henyey, LeLevier & Levee and of Ezer & Cameron, the unstable zone appeared only *late* in the evolution, and this is likely to be a result of the limited zoning of the interior structure which was employed in their models.

4. LABORATORY CONSIDERATIONS

Spiegel (1969) has summarized the relevant laboratory experiments on convectively unstable fluids. While a significant density gradient is unattainable in the laboratory and salt water is certainly not a hydrogen–helium gas, salinity experiments in heated water do suggest that the final state of convective neutrality is governed by the SH prescription (equation (7)). But the LSH criterion (1) seems to govern the rate at which the convecting layer in the laboratory experiments grows.

These results would tentatively indicate the validity of scheme S2/M2 or N2 in stars, since the assumed 'inner radiative zone' of the hybrid scheme N2 is definitely in radiative equilibrium if criterion (1) applies. On the other hand, if the convective growth rate is very slow in stars, it is possible that the hydrogen profile might be accordingly modified by criterion (1).

5. OBSERVATIONAL CONSIDERATIONS

Observational data for upper main-sequence stars (core hydrogen-burning phase) and supergiants (core helium-burning phase) can also shed light on the interior structure of massive stars and, in particular, on the distribution of mean molecular weight within their intermediate zones.

Upper main sequence

The H–R diagrams of the youngest clusters and associations show a distinct *turnoff* of the top of the main sequence, which runs either vertically or toward cooler effective temperatures and is reasonably well populated. While this fact is generally recognized in the case of the B associations, it is worth pointing out explicitly two typical examples among the O associations. In Per OB1, two turnoffs occur: one at Bo and the other at O5–O7 (Wildey 1964). In Sco OB1, two also occur: at O9–O9·5 and at O6–O7 (Schild, Hiltner & Sanduleak 1969). The stellar masses at the turnoffs range from $\sim 20\ M_\odot$ (Bo) to $\sim 60\ M_\odot$ (O5).

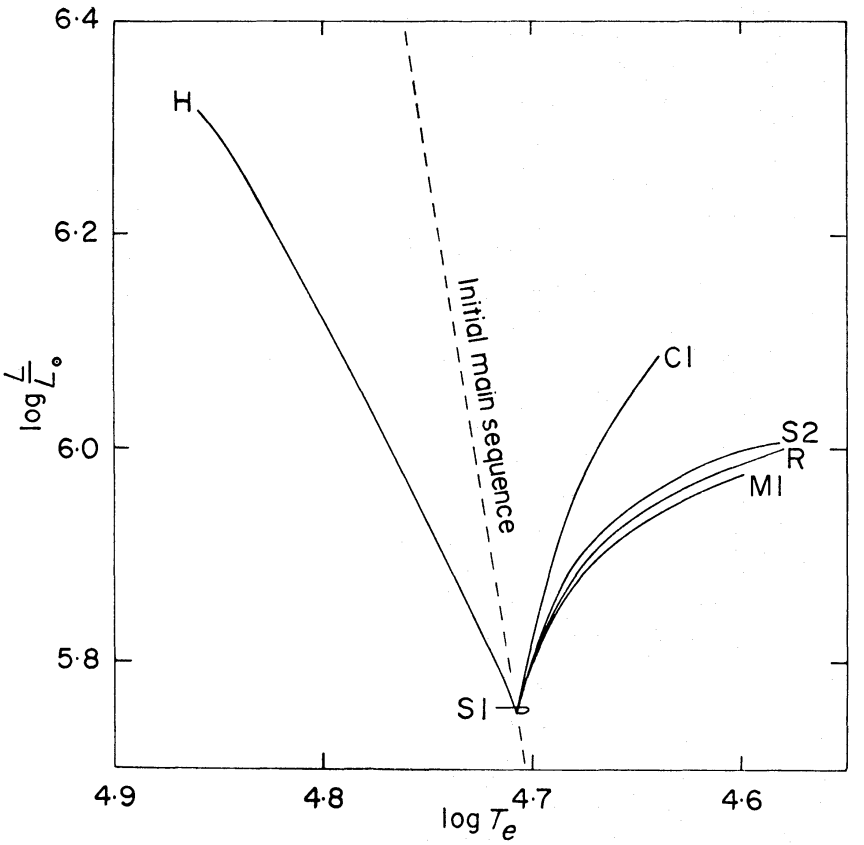

FIG. 4. *Theoretical H–R diagram for a star of* 60 $M_\odot$, *showing evolutionary tracks during core hydrogen burning for six schemes of evolution* (*cf. Fig.* 2).

A theoretical H–R diagram is shown in Fig. 4 for the purpose of comparison; the particular choice of 60 $M_\odot$ is not important since the behaviour of the tracks is qualitatively the same for any mass in the range 10–1000 $M_\odot$.* It is immediately seen that scheme H and scheme S1 may be ruled out on the basis of a predicted

* Indeed, the behaviour is qualitatively the same even for stars less massive than 10 $M_\odot$, as shown by calculations of Tayler (1956), who compared the only possible schemes R, H, and C1.

leftward track in the former case and of a predicted absence of any turnoff in the latter.

The lifetimes of core hydrogen burning for the various schemes are given in Table I. Although some of the lifetimes differ by as much as a factor of 2 at 60 $M_\odot$, the difference would be hard to detect observationally. Consideration of Figs 2–4 easily explains the trend of lifetimes at a given mass for the various schemes, if one recalls that

$$\tau = \int_{\bar{X}}^{X_e} \frac{EM}{L}\, d\bar{X}, \tag{8}$$

where

$$\bar{X} = \int_0^1 X\, dq$$

and E is the nuclear-energy release per gram due to the conversion of hydrogen into helium.

TABLE I

Core hydrogen-burning lifetime for certain of the evolutionary schemes (10^6 *yr*)

Scheme	15 $M_\odot$	60 $M_\odot$	1000 $M_\odot$	∞ $M_\odot$
R	—	3·1	—	1·4
H	—	3·8	—	1·4
C1	—	4·2	—	1·4
S1	—	2·1	1·5	1·4
S2	9·3	3·3	1·6	1·4
M1	9·1	3·1	1·6	1·4

Supergiants

For the supergiants, the general features of the H–R diagram provide another powerful test.

Scheme H will never result in any supergiants at all since the lack of internal chemical inhomogeneity prevents the necessary central condensation.

Schemes C1 and C2, as well as any hybrid schemes which cause the development of an extensive intermediate convection zone before core helium ignition, are characterized by *horizontal* hydrogen profiles in the intermediate zone and are known to cause contraction and burning of the helium core to take place only in the blue-supergiant region of the H–R diagram. The pertinent published models are based on the following schemes and masses: scheme C1 for the range 15–100 $M_\odot$ (Stothers & Chin 1968, cf. Sequence C of their paper); scheme C2 for 15 $M_\odot$ (Iben 1966); and scheme N2 for the range 20–50 $M_\odot$ (Morris 1969; Chiosi & Summa 1970, unpublished). Scheme N1 probably gives similar features on the H–R diagram because, in models for 30 $M_\odot$ in which this scheme was adopted for the last stages of core helium burning, the models tended to remain very blue compared with the models based on the previously adopted scheme M1. We conclude that, at least in models of supergiants more massive than $\sim$15 $M_\odot$, schemes C1, C2, N2, and probably N1 cause stars to avoid the red region until *after* core helium burning.

On the other hand, schemes R and M1, characterized by *diagonal* hydrogen profiles in the intermediate zone, cause core helium burning to begin in the red region and to terminate in the blue region. The relevant published models encompass the mass range 10–100 $M_\odot$ (Iinuma 1959; Stothers & Chin 1968).

Scheme M2 is presumed to produce the same result as schemes R and M1 because of the similar hydrogen profiles in the three cases.

Scheme S1 has not been calculated explicitly beyond the phase of core hydrogen burning, but will almost certainly result in the star's burning core helium *only* as a red supergiant because of the very small core size produced. According to the results of Stothers & Chin (1968) and Simon & Stothers (1969), the radius of a massive star is a sensitive function of the mass fraction contained in the helium core. Even at 60 $M_\odot$, the mass fraction of the core resulting from scheme S1 is far too small (despite allowance for its growth during hydrogen shell burning) to attain a size sufficient to make the stellar radius shrink. Thus, scheme S1 seems to be ruled out on the basis of the mere existence of blue supergiants of very high mass (Stothers & Simon 1968).

Schemes S2 and M2 must eventually develop into one of the convective hybrid schemes after the end of core hydrogen burning, as pointed out above. At this late stage, it is very probable that only a *small* convective intermediate zone would develop before helium ignition. This belief is reinforced by our knowledge that convective instability outside the core *vanishes* completely for all schemes at 15 $M_\odot$ before helium ignition, and that a convective intermediate zone becomes necessary in the case of scheme M1 for 30 $M_\odot$ only *after* helium ignition. A small convective intermediate zone would not prevent the star from becoming a red supergiant before helium burning.

To distinguish between the main 'convective' schemes (C1, C2, N1, and N2) and the surviving 'semiconvective' schemes (R, S2, M1, and M2), we require information on the *direction* of evolution across the H–R diagram during core helium burning. It now seems virtually certain that evolution proceeds from red to blue. The observational evidence for this comprises the following information, which is, however, pertinent only to the mass range 10–25 $M_\odot$ (Stothers 1969; Stothers & Chin 1969; Stothers & Evans 1970, unpublished): (1) the relative frequency of binaries among blue and red supergiants; (2) the relative numbers of blue and red supergiants: (3) the relatively large number of yellow supergiants with respect to the sum of blue and red supergiants; (4) the relative scarcity of luminous carbon stars; (5) the relative luminosities of blue and red supergiants; and (6) the observed abundance ratios of the CNO elements in blue supergiants. Potentially, the secular change of the effective temperature of blue and yellow supergiants (Liller & Liller 1965) and the fine detail of the distribution of blue and yellow supergiants on the H–R diagram (Stothers & Chin 1968) could also be used as tests, especially since *all* of the yellow supergiants should be cooling at an accelerated rate if the convective schemes were correct.

We conclude that the available observational evidence rules out evolutionary schemes H, S1, C1, C2, and any hybrid schemes with a *large* convective intermediate zone. (But schemes C1, C2, N1, and N2 cannot be ruled out in the case of masses higher than $\sim 25\ M_\odot$.) Thus a gentle hydrogen gradient in the intermediate zone seems to be required by the observations, such as is yielded by schemes R, S2, M1, and M2 or small modifications thereof.

6. CONCLUSION

Ten schemes have been discussed which attempt to predict the character of mixing and the resulting hydrogen profile inside the unstable intermediate zone of evolving main-sequence stars of high mass. New evidence, drawn from observa-

tional data and from a large number of stellar models, has been added to basic physical considerations and the available laboratory experiments in an effort to determine which scheme or schemes are fully consistent with all of the available evidence. Results for the ten schemes are summarized in Table II.

TABLE II

Summary of evidence concerning the possible treatments of the unstable intermediate zone during core hydrogen burning

Scheme	Physical	Laboratory	Consistency Observational	Models*
R	No	No	Possible	$< 10\ M_\odot$
H	No	—	No	ZAMS only
C1	No	—	No†	—
C2	No	—	No†	—
S1	Possible	No?	No	~ 25 to $> 1000\ M_\odot$
S2	Possible	Yes?	Possible	15 to $> 1000\ M_\odot$
M1	Possible	No?	Possible	10 to $> 1000\ M_\odot$
M2	Possible?	Yes?	Possible	10 to 15 $M_\odot$
N1	Possible	No?	No†	Not determined
N2	Possible	Yes?	No†	Not determined (but at least 20 to 50 $M_\odot$)

* No rotation; electron-scattering opacity; $X_e = 0{\cdot}70$, $Z_e = 0{\cdot}03$, $X_{CNO} = Z_e/2$.
† Refers to masses less than ~ 25 $M_\odot$.

We may draw conclusions from this table and from our earlier discussion as follows. Below 9 or 10 $M_\odot$, the intermediate zone develops without convective instability, and scheme R is appropriate. Above 9 $M_\odot$, a semiconvective zone develops whose chemical gradient is to be determined either by the LSH prescription (6) or by the SH prescription (7). During the earliest stages of core hydrogen depletion, the semiconvective zone probably connects smoothly the convective core and the outer radiative envelope (scheme S1 or S2). At some point during the subsequent stages, the semiconvective zone becomes detached from the core in order to conserve the radiative flux and the content of unburned hydrogen; a radiative zone then appears at the core boundary (scheme M1 or M2). For masses higher than 15 $M_\odot$ calculated with the SH prescription (scheme S2), the radiative zone does not appear until *after* core hydrogen exhaustion. Finally, a slight modification of the inner boundary of the detached semiconvective zone may occasionally involve the development of a *small* fully convective zone. In any event, the resulting hydrogen profiles based on schemes S2, M1, and M2 are very similar.

Although a clear choice between schemes S1/M1 and S2/M2 cannot be made at the present time, we wish to point out that the pertinent laboratory experiments tend to support scheme S2/M2.

ACKNOWLEDGMENTS

Drs C. Chiosi and C. Summa very kindly communicated their results in advance of publication. Dr D. Ezer is also thanked for providing additional details of her published models. Special thanks are due to Dr E. A. Spiegel for his careful and critical reading of the manuscript.

Institute for Space Studies, Goddard Space Flight Center, NASA, New York, U.S.A.
Received in original form 1970 *May* 12

REFERENCES

Blackler, J. M., 1958. *Mon. Not. R. astr. Soc.*, **118,** 37.
Chiosi, C. & Summa, C., 1970. Unpublished.
Ezer, D. & Cameron, A. G. W., 1967. *Can. J. Phys.*, **45,** 3429.
Gabriel, M., 1969. *Astr. Astrophys.*, **1,** 321.
Hartwick, F. D. A., 1967. *Astrophys. J.*, **150,** 953.
Henyey, L. G., LeLevier, R. & Levee, R. D., 1959. *Astrophys. J.*, **129,** 2.
Hoyle, F., 1960. *Mon. Not. R. astr. Soc.*, **120,** 22.
Iben, I., 1966. *Astrophys. J.*, **143,** 516.
Iinuma, Y., 1959. *Sci. Rep. Tohoku Univ.*, Ser. I, **43,** 232.
Kato, S., 1967. *Publ. astr. Soc. Japan*, **18,** 374.
Kippenhahn, R., 1963. *Star Evolution*, p. 330, ed. by L. Gratton, Academic Press, New York.
Kippenhahn, R., 1969. *Astr. Astrophys.*, **3,** 83.
Kushwaha, R. S., 1957. *Astrophys. J.*, **125,** 242.
Ledoux, P., 1947. *Astrophys. J.*, **105,** 305.
Levee, R. D. & Hilton, P. L., 1959. *Modèles d'étoiles et évolution stellaire* (*Mém. Soc. R. Sci. Liège*, Ser. 5, Vol. 3), p. 514.
Liller, M. H. & Liller, W., 1965. *Astrophys. J.*, **142,** 1028.
Morris, S. C., 1969. *Q. Jl R. astr. Soc.*, **10,** 274.
Paczynski, B., 1967. *Acta Astr.*, **17,** 355.
Percy, J. R., 1970. *Astrophys. J.*, **159,** 177.
Sakashita, S. & Hayashi, C., 1959. *Prog. theor. Phys.*, (Kyoto), **22,** 830.
Sakashita, S. & Hayashi, C., 1961. *Prog. theor. Phys.*, (Kyoto), **26,** 942.
Sakashita, S., Ono, Y. & Hayashi, C., 1959. *Prog. theor. Phys.*, (Kyoto), **21,** 315.
Savedoff, M. & van Dyck, S. R., 1959. *Modèles d'étoiles et évolution stellaire* (*Mém. Soc. R. Sci. Liège*, Ser. 5, Vol. 3), p. 523.
Schild, R. E., Hiltner, W. A. & Sanduleak, N., 1969. *Astrophys. J.*, **156,** 611.
Schwarzschild, M. & Härm, R., 1958. *Astrophys. J.*, **128,** 348.
Simon, N. R. & Stothers, R., 1969. *Astrophys. J.*, **155,** 247.
Spiegel, E. A., 1969. *Comments on Astrophys. Sp. Phys.*, **1,** 57.
Stothers, R., 1963. *Astrophys. J.*, **138,** 1074.
Stothers, R., 1965. *Astrophys. J.*, **141,** 671.
Stothers, R., 1966a. *Astrophys. J.*, **143,** 91.
Stothers, R., 1966b. *Astrophys. J.*, **144,** 959.
Stothers, R., 1968. *Nucleosynthesis*, p. 107, eds W. D. Arnett, C. J. Hansen, J. W. Truran & A. G. W. Cameron, Gordon & Breach Publishers, New York.
Stothers, R., 1969. *Astrophys. J.*, **155,** 935.
Stothers, R. & Chin, C.-W., 1968. *Astrophys. J.*, **152,** 225.
Stothers, R. & Chin, C.-W., 1969. *Astrophys. J.*, **158,** 1039.
Stothers, R. & Evans, T. L., 1970. Unpublished.
Stothers, R. & Simon, N. R., 1968. *Astrophys. J.*, **152,** 233.
Tayler, R. J., 1954. *Astrophys. J.*, **120,** 332.
Tayler, R. J., 1956. *Mon. Not. R. astr. Soc.*, **116,** 25.
Tayler, R. J., 1969. *Mon. Not. R. astr. Soc.*, **144,** 231.
Uchida, J., Suda, K. & Hitotuyanagi, Z., 1967. *Sci. Rep. Tohoku Univ.*, Ser. I, **50,** 8.
Unno, W., 1965. *Z. Astrophys.*, **61,** 268.
Van der Borght, R., 1964. *Aust. J. Phys.*, **17,** 165.
Wildey, R. L., 1964. *Astrophys. J. Suppl.*, **8,** 439.